Clim. Past Discuss., 8, 4779–4815, 2012
www.clim-past-discuss.net/8/4779/2012/
doi:10.5194/cpd-8-4779-2012

Climate of the Past Discussions

Testing the potential of OSL, TT-OSL, IRSL and post-IR IRSL luminescence dating on a Middle Pleistocene sediment record of Lake El'gygytgyn, Russia

A. Zander and A. Hilgers

University of Cologne, Institute of Geography, Cologne, Germany

Received: 18 September 2012 – Accepted: 19 September 2012
– Published: 28 September 2012

Correspondence to: A. Zander (anja.zander@uni-koeln.de)

Published by Copernicus Publications on behalf of the European Geosciences Union.

Abstract

Lake El'gygytgyn is a 12 km wide crater lake located in remote Chukotka in the far East Russian Arctic about 100 km to the north of the Arctic Circle. It was formed by a meteorite impact about 3.58 Ma ago. This study tests the paleomagnetic and proxy data-based Mid- to Late-Pleistocene sediment deposition history using novel luminescence dating techniques of sediment cores taken from the centre of the 175 m deep lake. For dating polymineral and quartz fine grains (4–11 µm grain size range) were extracted from nine different levels from the upper 28 m of sediment cores 5011-1A and 5011-1B. Polymineral sub-samples were analysed by infra-red stimulated luminescence (IRSL) and post-IR infra-red stimulated luminescence (post-IR IRSL) using single aliquot regenerative dose (SAR) sequences. SAR protocols were further applied to measure the blue light optically stimulated luminescence (OSL) and thermally-transferred OSL (TT-OSL) of fine-grained quartz supplemented by a multiple aliquot TT-OSL approach. According to an independent age model, the lowest sample from 27.8–27.9 m below lake bottom level correlates to the Brunhes-Matuyama (B/M) reversal. Finally, the SAR post-IR-IRSL protocol applied to polymineral fine grains was the only luminescence technique able to provide dating results of acceptable accuracy up to ca. 700 ka. Major factors limiting precision and accuracy of the luminescence chronology are, for some samples, natural signals already approaching saturation level, and overall the uncertainty related to the sediment water content and its variations over geological times.

1 Introduction

Luminescence dating is long established as a reliable tool to provide absolute chronologies for Late Pleistocene sediments from numerous depositional environments. The event being dated by luminescence is the exposure of the sediments to sunlight prior to deposition and coverage. Most dating studies are based on quartz optically stimulated luminescence (OSL) applied on sediment archives of aeolian, fluvial or lacustrine

CPD
8, 4779–4815, 2012

origin. However, the use of quartz for OSL dating is typically limited to the last 100–150 ka because of saturation effects of the quartz luminescence signal with increasing dose. Infrared stimulated luminescence (IRSL) of potassium-rich feldspars has the potential to extend the datable age range because dose-response curves from K-rich feldspars or polymineral fine grains show a much higher saturation dose compared to quartz. But it has been known for several decades now that the IRSL signal can show anomalous fading (Wintle, 1973). This signal loss over burial time often gives rise to significant age underestimation. Fading correction procedures have been developed (Lamothe and Auclair, 1999; Huntley and Lamothe, 2001) to correct for these underestimations but they are inapplicable at samples, in which dose response curves advance the saturation level. Recent studies (Thomsen et al., 2008; Buylaert et al., 2009; Li and Li, 2011) have presented a measuring protocol, in which a high temperature IRSL signal is measured after a low temperature IRSL signal. This post-IR IRSL is less prone to fading but has the same high saturation dose limits as the low temperature IRSL. These characteristics make this a method of great importance for dating Middle and Late Pleistocene deposits and it has become the preferred protocol for feldspar dating if fading corrections are unreliable or not valid (Buylaert et al., 2012).

Only very few studies have focussed on luminescence dating of lake sediments from the Upper and Middle Pleistocene so far (e.g. Forman et al., 2007; Juschus et al., 2007; Lowick and Preusser, 2011; Lukas et al., 2012). This is probably due to the fact that such environments are afflicted with several complications. One important complication is the accurate estimation of the palaeo-water content. This variable is the most crucial, because water attenuates external radiation and causes a lowering of the dose rate received by the dosimeters, i.e. the sediment grains. The dose rate is a substantial part of the age equation and faulty dose rate calculations lead to inaccurate ages. A second problem that can affect the dose rate determination in lacustrine environments is the presence of radioactive disequilibria in the uranium decay chain (Krbetschek et al., 1994). Similar to changes in water content, this imparts a non-constant dose rate on the sampled material through time. A third question that has to be considered comprises

CPD
8, 4779–4815, 2012

the potential sediment transport processes and remobilisation processes by turbidites or landslides.

Lake El'gygytgyn is located in Central Chukotka, NE Russia, ∼ 100 km north of the Arctic Cycle (Fig. 1) and even today the surface is frozen and covered with ice for about 9 months of the year (Melles et al., 2012). Fluvial and aeolian input is thus limited to the few summer months when the lake surface is open water and the light conditions allow a reasonable bleaching of the sediment grains. However, the crater is roughly 18 km in diameter and the catchment is less than three times the lake's surface area (Melles et al., 2011). About 50 small inlet streams drain into the lake (Nolan et al., 2002) and it is relevant if the distance of just a few km is sufficiently long to enable full bleaching of the transported sediment. Today, the fluvial input to the lake is very low and much of the sediment is deposited at the mouth of the inflows in shallow lagoons, which are dammed by gravel bars formed by wave and lake ice action (Melles et al., 2011). Temporary deposition in these lagoons and further transport through the clear surface waters, giving a Secchi transparency depth of 19 m in summer (Melles et al., 2012), might enable a reasonable bleaching of the suspended matters. In addition, as a result of short transport distances, sediments may have experienced insufficient cycling prior to deposition, which may lead to poor OSL-sensitivity in quartz samples (Preusser et al., 2006; Fuchs and Owen, 2008), which in turn makes extraction of a dateable signal sometimes challenging.

The samples analysed in this study originate from cores A and B of ICDP site 5011, which was drilled from February until April 2009 employing a 100 tons drilling platform on the artificially thickened ice cover in 170 m water depth in the central part of Lake El'gygytgyn (Melles et al., 2011; Fig. 1). An independent age model for the 3.6 Ma core composite is provided by magnetostratigraphy and tuning of proxy data to the regional insolation and global marine isotope stratigraphy (Melles et al., 2012; Nowaczyk et al., 2012). The objective of our study was to test different approaches of luminescence dating on the exceptionally long sediment record drilled, and provide complemental information on the core stratigraphy.

CPD
8, 4779–4815, 2012

2 Sample preparation

The cores from ICDP site 5011 were taken in transparent plastic liners of 10 cm diameter. For luminescence dating, 10 cm thick pieces were taken from replicate core parts and wrapped with black tape to prevent further light exposure. These liner pieces were then opened under subdued red-light conditions in the luminescence sample preparation laboratory in Cologne. The sediment was pushed out of the liner and a small block of 3 × 3 × 6 cm was cut out of the inner core to eliminate any grains that were exposed to light during cutting and preparing of the liner pieces. The small block was then treated with hydrochloric acid, hydrogen peroxide and sodium oxalate to remove carbonate, organics and dissolve coagulations. Due to the lack of sufficient sand-sized minerals, the 4–11 µm fine grain fraction was prepared following Frechen et al. (1996). Quartz was separated by etching the polymineral fine grains with hexafluorosilicic acid for 7 days.

The remaining sediments from the liner were dried, homogenised and prepared for gamma-ray spectrometry. The effective water content was determined by weight loss after drying the bulk samples and is given in relation of weight water to dry mass. Comparing the results with the original water content, measured at a second correlative core soon after drilling, most of the values are in fairly good agreement (Table 1), indicating that no significant water loss has happened between coring and sample preparation. Only sample 1A1H3, taken from a turbidite layer, shows a significant discrepancy.

3 Dosimetry

Radionuclide analyses (uranium, thorium, potassium) were carried out by gamma-ray spectrometry in the Cologne laboratory and at the VKTA Rossendorf e.V. (D. Degering, Dresden), respectively (see Table 1). 157 g of dry sample material was packed in 90 × 25 mm polystyrol containers and stored for 4 weeks to compensate for radon loss induced by sample preparation.

CPD
8, 4779–4815, 2012

In water-lain sediments disequilibria in the uranium decay series are quite common. The impact of changes in the sediment dose rate on age estimates can be substantial but is hardly quantifiable over large time scales. An underestimation of dose rate compared to the effective dose rate over the whole time period of burial would result in an age overestimation. The Cologne gamma-ray spectrometer has a good sensitivity in the higher energy part of the spectrum and ^{238}U is hence quantified by peaks of ^{226}Ra, ^{214}Pb and ^{214}Bi, emitting gamma radiation beyond 100 keV. The high resolution gamma-spectrometer in Dresden has good sensitivity in the lower energy spectrum and can quantify ^{234}Th, which directly follows the mother isotope ^{238}U and has its main emissions at 63 and 93 keV. Comparing the $^{238}U/^{234}Th$ with ^{226}Ra provides more information about disequilibria in the early decay chain and can reveal uranium loss or uptake since uranium is mobile in oxidising aqueous solutions. Radium is also known to be mobile in lake sediments and can accumulate in individual horizons. The samples analysed in Dresden show only a small decrease between the early isotopes and ^{226}Ra but two of the three samples show a slightly more significant decrease between ^{226}Ra and ^{210}Pb (Fig. S1). This indicates a radon loss and may give evidence for the uranium series not being in the state of equilibrium. However, for all the three samples analysed here the activities of the daughters ^{226}Ra and ^{210}Pb still agree within 2-sigma errors with the activity of the mother (Fig. S1). Hence, the impact on age calculation is presumably not massive. With regard to the decay rates of the nuclides this decrease can be attributed to mobilisation processes within the last about 100 yr but it is not possible to quantify the frequency of the mobilisation processes over the last several hundred thousand years and, therefore, it is not viable to qualify the real impact on the age calculation.

Dose rates (see Tables 3 and 6) and ages were calculated using the "age" software (version 1999) by R. Grün, Canberra, which includes the dose conversion factors published by Adamiec and Aitken (1998). Alpha efficiency was set to 0.035 ± 0.02 for quartz samples and 0.07 ± 0.02 for polymineral fine grain samples, following Rees-Jones (1995).

CPD
8, 4779–4815, 2012

3.1 Attenuation factors and water content

The cosmic contribution to the dose rate is usually calculated according to the sampling depth. It can be neglected for the given samples, because the influence of cosmic radiation on the minerals is completely attenuated by overlying sediment and water column. More important is the impact of the sediment water content. Attenuation of ionising radiation is more effective in sediments with water-filled interstices and has strong effects on resulting age estimates. The "as found" water contents are hardly representative for the moisture conditions during the time span of burial, especially not for such a long period of time as considered in this study. Mechanical compaction by overlying sediments and mass movements may have reduced or increased the water content during burial times and are difficult to quantify. Full saturation of the sediment can be measured using laboratory methods (Lowick and Preusser, 2009) but a retrospective determination of water content changes through time is far from being straightforward. We therefore took the measured water content for age calculation and added three more age estimates calculated with fictive water contents in the tables to illustrate the impact of water content variation on age calculation (see Tables 3 and 6).

4 Luminescence measurements and results

Luminescence measurements were carried out on an automated Risø TL/OSL Reader (TL-DA 12) with a calibrated $^{90}Sr/^{90}Y$ beta source delivering 4.08 Gy min^{-1}. A U340 filter was used for quartz measurements and an interference 410 nm filter for IRSL measurements on polymineral samples. Several different dating techniques had to be tested in this study to evaluate the most appropriate protocol for achieving reliable luminescence age estimates for such old, i.e. > 300 ka, sediments (Table 2). This expanded dating programme evolved from the fact that the sediments analysed here are comparably old and cover a time span which is not often securely dated by luminescence techniques.

CPD
8, 4779–4815, 2012

4.1 SAR-OSL on fine grain quartz

The standard SAR protocol (Murray and Wintle, 2000) was applied on three samples, using blue stimulation for 50 s at 125 °C, a pre-heat of 240 °C and a cut heat of 220 °C. Equivalent dose (D_e) values were determined using the first 0.6 s of the OSL decay curve, and subtracting the background of the last 5 s. Another approach using the early background subtraction method (Ballarini et al., 2007) with an integral of 0–0.4 s for D_e determination and a background integral of 1.0–1.4 s, as described by Lowick and Preußer (2011), did not improve the dataset and was hence rejected. Dose response curves were fitted with a single exponential plus linear function. An experimental dose-response curve measured for sample 1B2H2 with 12 dose steps up to a 1237 Gy fitted well to a single saturated plus linear function and did not show any saturation effects (Fig. 2). Validation of the protocol parameters was verified by pre-heat plateau tests and dose recovery tests at different temperatures. The validation tests both confirmed an appropriate pre-heat temperature between 220 °C and 240 °C and a perfect dose recovery at 240 °C with a measured to given dose ratio of 1.00 (Fig. 3a and b). IR tests for feldspar contamination were made standard practice.

The results obtained for the standard SAR-OSL protocol on quartz underestimate the expected age range significantly. Maximum D_e-values remained below 410 Gy and none of the three samples reached the saturation level. The maximum D_e was obtained for sample 1A6H1B. With regard to the age model provided by Melles et al. (2012) and Nowaczyk et al. (2012) sample 1A6H1B from 17.88–17.93 m blf (below lake floor) is supposed to be deposited about 465 ka ago. Sample 1A9H2 was taken between 27.817–27.917 m blf and is supposed to be 757 ka years old. The SAR-OSL results of 137 ± 20 ka and 129 ± 13 ka for these two samples are far below the expected age range and show no increase in age with depth (Table 3 and Fig. 5). Although the dose response curves show no saturation effects with increasing dose, 400 Gy appears to be the maximum D_e for fine grain quartz. Thus, a quartz age beyond 200 ka is not attainable.

CPD
8, 4779–4815, 2012

Although the SAR-OSL protocol is the most accepted protocol and has proved very successful when dating quartz, there are several studies reporting age underestimations for quartz beyond the Eemian or even as young as 70 ka (Murray et al., 2008). Similar observations were made by Lowick and Preusser (2011), Lowick et al. (2010), Lai (2010), Timar et al. (2010), who all reported on underestimations with fine grain quartz. The majority of these studies show that the samples meet the standard validation criteria for the SAR protocol, which usually allows the assumption to obtain reliable OSL ages. They all observed well-shaped dose response curves, which are best fitted to a single exponential plus linear function. While the characteristics of the dose response curve suggested that determination of D_e-values up to 400 Gy should be possible, Lai (2010) showed that age determination was only reliable up to 230 Gy. Lowick and Preusser (2011) and Lowick et al. (2010) reported on sedimentary quartz from Northeastern Italy. Their OSL ages agree well with biochronological constraints up to 140 Gy (70 ka) but increasingly underestimate the age beyond this point. They assume the underestimations are caused by the presence of different components of luminescence signals with different luminescence characteristics but have no real explanation for them. They also report on the slow growing dose response curve beyond 400 Gy, which is represented by a linear component.

A decomposition of the L_x/T_x quotient from our study revealed an obvious answer to the question, why the dose response curve shows a linear response to high doses. Plotting the background-subtracted regenerated signals (L_x) and the background-subtracted test dose signals (T_x) against the administered beta dose shows a saturation of the L_x-curve above 400–500 Gy. The corresponding test dose signal (T_x) shows a small rise up to the 500 Gy regenerative dose and a decrease beyond, although the test dose was always kept constant (Fig. 2). The ratio then seems to indicate a rising L_x/T_x with dose but the uncorrected OSL signal is in saturation. Hence, signal growth of the sensitivity-corrected OSL signals is an artefact of the response to the test dose that is commonly well below the saturation level. Here, sensitivity correction as conducted as part of the SAR protocol results in erroneous equivalent dose estimates in dose ranges beyond the saturation level of the uncorrected regenerated OSL.

4.2 Thermally transferred OSL (TT-OSL)

Thermally transferred OSL (TT-OSL) was proposed by Wang et al. (2006) to extend the age range of quartz and to provide quartz OSL dates for Middle Pleistocene sediments. The TT-OSL signal is measured after the depletion of the conventional OSL signal and a subsequent pre-heat, which is applied to induce the thermal transfer of charge. The TT-OSL signal has a saturation limit at least an order of magnitude greater than the fast component of the conventional OSL signal (Wang et al., 2007) but, in contrast to initial suggestions by Wang et al. (2006), it is considerably less light sensitive than the fast bleaching OSL component (Tsukamoto et al., 2008; Jacobs et al., 2011). The simplified SAR protocol for TT-OSL developed by Porat et al. (2009) (Table 2) was tested on 3 different samples but results showed that it was not suited for the quartz from Lake El'gygytgyn. Significant sensitivity changes and a non-linear dose response prevented the fitting of a sensible dose response curve to the data. A dose recovery test carried out on 1A3H1 failed to meet the validation criteria; the average measured dose overestimated the given dose by more than 25 % and resulted in a ratio of 1.32. The recycling ratio was poor (more than the acceptable 10 % deviation) and the recuperation of 10–20 % was significantly exceeding the acceptance level of 5 % (Murray and Wintle, 2000). An additional hot bleach (OSL shine down at 300 °C for 100 s), as proposed by Stevens et al. (2009), was then added after the TT-OSL measurement to remove the residual charge carried over from the regenerated dose measurements to the test dose measurement cycle. This lead to a perfectly linear dose response curve (Fig. 4), however, the overestimation was hardly reduced, the recycling ratio remained poor, and the recuperation still varied between 4 % and 10 %. Independent tests of this modified TT-OSL protocol applied on modern test quartz with an artificial beta dose of 206 Gy yielded a perfect linear growth curve, a very small underestimation of about 5 %, and a given to measured dose ratio of 1.05. The average recycling ratio was within

10 % deviation and the recuperation was negligible. This result underlines the general validity of the modified TT-OSL protocol, but also that it is not suitable for the samples of this study.

To avoid the problem of charge transfer a multiple aliquot regenerative dose (MAR) TT-OSL approach was designed and tested. Twelve and 16 discs, respectively, were prepared from two samples (see Table 3). The natural OSL and the natural TT-OSL (step 2–5 from the given SAR protocol, Table 2) were recorded and followed by a hot bleach (300 s blue stimulation at 280 °C). The same discs were then irradiated with 4 dose steps up to 814 Gy and step 2–5 from the SAR protocol were repeated. The first 0.4 s of the natural TT-OSL signal were used for short shine normalisation and the residual level was determined by repeating step 2–5 on the first three discs. D_e-values were determined by integrating the first 1.2 s and the average signal of the last 10 s was subtracted for background. The results show a linear growth curve and a good response to the short shine normalisation. Sample 1A1H3 overestimates the expected age range that is inferred from independent age model if the measured water content, which is comparably high, is used for age calculation. A water content of about 70 %, as measured for many of the other samples, would yield an age of about 160 ka. This would match the expected age range and gives a good example for the impact of the water content on the age calculation. The result of sample 1A4H2, however, underestimates the expected age range significantly (see Table 3). Hence, with respect to the independent age control TT-OSL protocols were considered not to yield the required reliability for dating the samples under study here.

4.3 SAR-IRSL$_{50}$ on polymineral fine grain

The SAR-IRSL$_{50}$ protocol (Table 2) proposed by Wallinga et al. (2000) for coarse grain feldspars was slightly modified and applied on the polymineral fine grain fraction. This fraction contains the natural fine silt mineral composition including quartz, though the IR stimulated luminescence emitted in the 410 nm range is dominated by potassium-rich feldspar. Feldspar is known to have a much higher saturation dose than quartz and is therefore often used if quartz is not suited for various reasons. However the available age range and the precision of feldspar dating is often hampered by anomalous fading, a spontaneous signal loss (Wintle, 1973) that leads to age underestimations of feldspar ages. Corrections for this signal loss and the corresponding age underestimations have been proposed (Lamothe and Auclair, 1999; Huntley and Lamothe, 2001), but these corrections are not valid for old samples with large palaeodoses and, hence, non-linear dose response curves.

IRSL measurements were carried out for 350 s at 50 °C ($IRSL_{50}$) through an interference filter (410 nm, 5 mm). Dose recovery pre-heat tests were conducted to determine the appropriate pre-heat temperature and to verify the protocol parameters. A set of 15 sub-samples of sample 1A1H2 received a hot bleach, i.e. a 100 s IRSL stimulation at 280 °C in the reader and a subsequent beta dose of 206 Gy. Three discs each were measured at different pre-heat temperatures using the same thermal treatments for the regenerative dose and the test dose. The average D_e's obtained for the different pre-heat temperatures show no plateau (Fig. 5), but a constant decrease with temperature and only a presumably accidental match of the administered dose at a pre-heat temperature of 230 °C. In addition, the D_e is strongly dependent on the integral size used for D_e calculation showing a constant increase of about 17 % within the first 25 measurement channels. This performance is usually taken as evidence for signal instability, i.e. for fading, but fading tests revealed only very small fading rates of $1.2 \pm 0.4\,\%\,\text{decade}^{-1}$ (1B3H2) and $0.6 \pm 0.4\,\%\,\text{decade}^{-1}$ (1A3H1). Summarising these observations, the polymineral fine grains are not suitable for the standard SAR-$IRSL_{50}$ dating protocol. With regard to the insufficient pre-heat plateau, any dating approaches were abandoned because the obtainable results would at best be minimum ages which underestimate the true deposition age significantly. Using polymineral fine grain from younger Lake El'gygytgyn sediments, Juschus et al. (2007) and Forman et al. (2007) described only small fading rates and they forebear from doing fading corrections. They obtained a good agreement with the expected age range up to ∼ 160 ka, but underestimate the expected age range significantly beyond 160 ka (Forman et al., 2007).

CPD
8, 4779–4815, 2012

4.4 Post-IR IRSL ($pIRIR_{290}$) on polymineral fine grain

Recent studies published by Thomsen et al. (2008) and Buylaert et al. (2009) described a high temperature IRSL signal, which is measured at increased temperatures after a first IR shine down. This post-IR IRSL signal appears to be less prone to fading and is more stable than the low-temperature IRSL signal measured at 50 °C ($IRSL_{50}$). The $pIRIR_{290}$ protocol (Table 2) proposed by Thiel et al. (2011) for middle and upper Pleistocene loess from Austria was applied on 8 of the polymineral fine grain samples. All sub-samples were prepared on aluminium discs and all measurements were made on a Risø TL-DA-12 with a 5 mm 410 nm interference filter. Thiel et al. (2011) integrated the first 2.4 s for D_e determination. With regard to a weak scatter that was observed at some sub-samples within the first 6–8 channels in the D_e vs. stimulation time-plot, the integral of 1–12 s was taken for D_e determination and the last 20 s were subtracted as background. In contrast to the SAR-$IRSL_{50}$ measurements, which showed an increasing D_e with increasing integral, the D_e of the high temperature $pIRIR_{290}$ does not depend on the size of the integral but shows an extended plateau up to approximately 30 s. With regard to the small number of sub-samples measured (Table 5), the median of the individual measurements was finally used as best representative for the average equivalent dose. Relating to the bleaching experiments, the signal left after bleaching for 3 h under natural sunlight (20 Gy) was subtracted from the $pIRIR_{290}$ D_e's (for discussion see also Thiel et al., 2012; Buylaert et al., 2012). All data are given with total uncertainties at a 1-sigma confidence level.

Thomsen et al. (2008) and Buylaert et al. (2009) have demonstrated that the post-IR IRSL signal is easy to bleach down to a certain residual level of 10–20 Gy, but that it is necessary to verify this assumption, since bleaching characteristics are strongly dependent on the sediment type and mineralogy of the feldspars. A sample set of 1A1H2 was prepared and bleached for 3.15 h and 7.5 h under natural sunlight on a bright cloudless day in June. Another sample set was bleached in a Höhnle solar simulator for 4.5 h, 6.5 h and 36 h. The results (Table 4) confirm that the $pIRIR_{290}$ signal is generally easy

CPD
8, 4779–4815, 2012

to bleach, even if the low temperature IRSL signal (L_x), which is measured prior to the pIRIR$_{290}$ signal (see Table 2), is bleached a little faster. After 3.5 h under natural sunlight the pIRIR$_{290}$ D_e of sample 1A1H2 is already reduced to about 20 Gy and it keeps decreasing with further exposure time. Artificial bleaching of different samples in a Höhnle solar simulator for 4.5, 6.5 h and 36 h gives a residual below 20 Gy. After 36 h in a solar simulator there is still a residual of 14 Gy, but the bleaching level is sample dependent and not only dependent on the bleaching time. However, this experiment illustrates that the post-IR IRSL signal of the lake sediments can be bleached to a reasonable level in a reasonable time.

The impact of these residuals on the ages can be considered to be quite low. For example, the residual of 20 Gy measured after 195 min of sunlight bleaching for sample 1A1H2 (see Table 4), corresponds to 7.7 ka using the dose rate based on the measured water content. The pIRIR$_{290}$ age of this sample is 179 ± 20 ka after subtraction of the residual. Thus, the residual is only 4 % and within the range of the 1-sigma error in age.

Dose recovery tests at 1A1H2 after a natural sunlight exposure for 450 min and a given dose of ∼ 470 Gy failed to pass the criteria. After subtracting the residual of 14 Gy the measured to given dose ratio was still 1.38 ± 0.09, but a valid protocol should be able to deliver a ratio within 10 % deviation from unity. Another dose recovery test was carried out on five discs of sample 1A3H2 after 390 min light exposure in the solar simulator and an artificial beta dose of ∼ 300 Gy. The measured to given dose ratio was still 1.37 ± 0.06, showing a massive overestimation, too. A further dose recovery test on sample 1A3H1 was carried out after 2160 min bleaching in the solar simulator. The sub-samples were stored for 6 months after bleaching, then received a beta dose of ∼ 300 Gy and the average measured to given dose ratio was 1.07, which is within the 10 % range and thus acceptable. Fife other discs of sample 1A3H1 and 1A3H2 received a hot bleach in the reader (step 7–10 of the protocol) instead of an optical bleach, a beta dose of ∼ 300 Gy and were then measured. The measured to given dose ratio was 0.99 ± 0.01 for 1A3H1 and 0.95 ± 0.01 for 1A3H2, thus passing the validity test. The other two routine tests, which are commonly checked by default, gave excellent results, illustrating that the sensitivity correction of the protocol is working well. The average recycling ratio was 1.03 ± 0.02 and the recuperation was low, ranging between 1.0 and 1.5 %. The results obtained for the dose recovery tests using optical bleaching immediately followed by a beta dose seem to indicate some kind of charge transfer after irradiation and during the first pre-heat. Although the natural signal is thoroughly bleached after a few hours under natural or artificial sunlight (Table 4), it is not possible to recover a given dose if measured immediately after bleaching. The resulting D_e overestimates the given dose significantly. If the sample is stored for some months after bleaching, the overestimation is reduced and the given dose can be recovered within 10 % deviation. Cleaning out the samples with a hot bleach before the first beta dose yields acceptable dose recovery ratios, suggesting no significant charge transfer or recuperation processes. At this stage, we do not have satisfactory explanation for the different behaviours with and without delay between bleaching and irradiation. We interpret this charge transfer observed after optical bleaching and immediate radiation as a laboratory artefact, which is not relevant for natural samples because under natural conditions bleaching and dosing will happen much slower. However, further experiments with varying pause times between bleaching, artificial irradiation and first pre-heat are necessary to analyse these observations in more detail.

5 Discussion on pIRIRSL$_{290}$ results

From the comparison of the luminescence dates with the independent age model it becomes evident that only the post-IR IRSL protocol yielded reliable dating results significantly beyond 200 ka (Table 6). The pIRIR$_{290}$ D_e-values (Table 5) show – in contrast to the IRSL values measured at 50 °C – a constant increase with depth. Three of the samples are in very good agreement with the expected age range, if the measured water content is used for age calculation. Samples from the age range between 200 and 300 ka overestimate the expected age range significantly (Fig. 6) by about 30 %. Many reasons are conceivable for this, such as saturation effects as visible for sample

CPD
8, 4779–4815, 2012

1A3H2, erroneous water contents or dose rate underestimation by means of disequilibria or even insufficient bleaching. Juschus et al. (2007) described decreasing water contents with depth for their sediment core with minimum values around 50 % at the base. There is no such trend visible for the samples of this study and the question remains if the measured water content represents the environmental conditions during the geological times since deposition.

The samples from the lower part of the profile are in good agreement with the expected age and even sample 1A9H2 from the B/M boundary with an expected natural dose of > 2700 Gy gave a D_e of more than 2400 Gy (Fig. 7) and an age of > 700 yr (Fig. 6). The dose response curves are best fitted to an exponential plus linear function and the natural sensitivity corrected signals exceed the highest regenerated dose point of 2430 Gy. The D_e obtained for 1A9H2 lies in the extrapolated part of the dose response curve and the true saturation level was not reached. D_e and age are hence just given as minimum values. In this part of the core section, the natural signal of the post-IR IRSL is slowly approaching the saturation level, but the dose response curve is rather steep compared to sample 1A6H1B (Fig. 7). Saturation dose experiments with up to 7 regeneration dose points and a maximum dose of 2500 Gy carried out on sample 1A6H1B and 1A4H2 still allow to fit an exponential plus linear function to the data but the natural $pIRIR_{290}$ signal lies in the upper slow rising linear part of the dose response curve and is close to saturation (Fig. 8). This slow rise considerably limits the reliability of the three samples 1A9H2, 1A4H2B and 1A3H2 and is taken as one of the reasons for the comparably large relative standard deviation observed for these samples. Polymineral fine grain samples usually do not show a significant scatter because a large number of grains on the sample disc are emitting luminescence signals. The $pIRIR_{290}$ D_e data sets of these samples show RSD-values between 18 % and 29 % (Table 5). Even if the number of aliquots is small and the validity is limited, this scatter is most likely ascribed to the shape of the dose response curve, indicating a natural dose close to saturation level. The scatter for the IRSL measurements at 50 °C is much smaller.

Discussion Paper | Discussion Paper | Discussion Paper | Discussion Paper |
CPD
8, 4779–4815, 2012

Testing the potential of OSL, TT-OSL, IRSL and post-IR IRSL luminescence dating

A. Zander and A. Hilgers

A similar dating approach by Thiel et al. (2011) on polymineral fine grains extracted from Austrian loess from below the B/M boundary was not successful because the natural of the $pIRIR_{290}$ signal was in the saturating part of the dose response curve, which they defined as > 1600 Gy. In our study the $pIRIR_{290}$ saturation dose was not reached up to 2400 Gy for sample 1A9H2, which is correlated to the B/M boundary. D_e-values derived for the low temperature IRSL signal measured as part of the $pIRIR_{290}$ measurement sequence (see Table 2) do not exceed a maximum value of 540 Gy (see Table 5). Whereas $pIRIR_{290}$ D_e-values continue to rise with depth, the low temperature IRSL ages show no increase with depth, which further illustrates the unreliability of these estimates (Table 6). A similar trend was described by Forman et al. (2007), who reported on significant underestimations beyond 160 ka for multiple aliquot low temperature IRSL measurements on polymineral fine grains. Finally, we deduce that the predominant agreement with the age model and the continuous age increase with depth (see Table 6) seem to speak for the validity of the $pIRIR_{290}$ data.

No fading corrections were made, neither for the $IRSL_{50}$ nor the $pIRIR_{290}$ D_e-values. Juschus et al. (2007) reported on small fading ratios between 0.84 and 0.99 and followed Forman et al. (2007), who determined fading ratios between 0.92 and 0.99 and did not apply fading corrections. The same trend was observed for two samples from this study, which gave fading rates of $1.2 \pm 0.4\,\%\,\text{decade}^{-1}$ (1B3H2) and $0.6 \pm 0.4\,\%\,\text{decade}^{-1}$ (1A3H1) for $IRSL_{50}$. Although these rates are small, an influence cannot be excluded. However, the introduced uncertainties associated with fading corrections in the considered age range are supposed to exceed any advantage of correction here. Buylaert et al. (2012) calculated fading rates for low temperature IRSL and post-IR IRSL at samples of different origins and concluded that fading rates of 1–1.5 % decade^{-1} are most likely artefacts of measurement procedures. We, hence, have abandoned any fading corrections for $IRSL_{50}$ and $pIRIR_{290}$ dose estimates.

Discussion Paper | Discussion Paper | Discussion Paper | Discussion Paper |

CPD

8, 4779–4815, 2012

Testing the potential of OSL, TT-OSL, IRSL and post-IR IRSL luminescence dating

A. Zander and A. Hilgers

6 Conclusions

The samples from Lake El'gygytgyn turned out to be very challenging for luminescence dating and the reasons therefore are manifold. Although the general luminescence properties of the sample material, like signal intensity, recuperation, dose response, sensitivity, and others, are acceptable for the fine-grained quartz and polymineral fractions, respectively, the SAR protocol for OSL and $IRSL_{50}$ dating techniques failed to deliver satisfactory and reliable dating results. Quartz OSL results underestimate the palaeomagnetic time frame significantly, for example date the sample from the 780 ka B/M boundary to only about 150 ka. A single aliquot TT-OSL protocol was inappropriate because insufficient sensitivity corrections prevented a reliable curve fit. A multiple aliquot TT-OSL protocol for fine grain quartz was tested, but failed for the older samples as well. The low temperature IRSL at 50 °C measured prior the high temperature IRSL at 290 °C during the $pIRIR_{290}$ sequence gave a maximum age of 180 ka, showing no age increase with depth.

Only post-IR IRSL measurements with 290 °C stimulation temperature ($pIRIR_{290}$) have passed all validation tests and result in ages that increase with depth down to the B/M boundary. Four out of eight samples are in fairly good agreement with the ages calculated from the magnetic polarity, though their errors are large. However, the results obtained for the uppermost sample and the samples from the MIS 7 sediment record seem to show systematic overestimations but still an increase in age with depth. It is not possible to verify if this overestimation is partly due to insufficient bleaching. Polymineral fine grain measurements do not allow conclusions about the bleaching level prior to deposition. Thus, for verification of the dating results obtained in this study it might be interesting for further projects to analyse the effective bleaching of a modern sample from the delta of one of the small inlet streams of Lake El'gygytgyn.

Discussion Paper | Discussion Paper | Discussion Paper | Discussion Paper |

CPD

8, 4779–4815, 2012

Testing the potential of OSL, TT-OSL, IRSL and post-IR IRSL luminescence dating

A. Zander and A. Hilgers

Supplementary material related to this article is available online at: http://www.clim-past-discuss.net/8/4779/2012/cpd-8-4779-2012-supplement.pdf.

Acknowledgements. Funding for the "El'gygytgyn Drilling Project" was provided by the International Continental Scientific Drilling Program (IPDP), the US National Science Foundation, the German Federal Ministry of Education and Research (BMBF; grant 03G0642), Alfred Wegener Institute (AWI) and GeoForschungsZentrum (GFZ), the Russian Academy of Sciences Far East Branch (RAS-FEB), the Russian Foundation for Basic Research (RFBR), and the Austrian Federal Ministry of Science and Research (BMWF). The Russian GLAD 800 drilling system was developed and operated by DOSECC Inc., and LacCore, at the University of Minnesota, handled core curation. Financial support for the luminescence dating was provided by the BMBF. We thank all participants on the drilling operation and on the core subsampling at the University of Cologne for their competent help and collaboration. Water content measurements as listed in Table 1 were contributed by V. Wennrich.

References

Adamiec, G. and Aitken, M. J.: Dose-rate conversion factors: update, Ancient TL, 16, 37–49, 1998.

Ballarini, M., Wallinga, J., Wintle, A. G., and Bos, A. J. J.: A modified SAR protocol for optical dating of individual grains from young quartz samples, Radiat. Meas., 42, 360–369, 2007.

Buylaert, J.-P., Murray, A. S., Thomsen, K. J., and Jain, M.: Testing the potential of an elevated temperature IRSL signal from K-feldspar, Radiat. Meas., 44, 560–565, 2009.

Buylaert, J.-P., Jain, M., Murray, A. S., Thomsen, K. J., Thiel, C., and Sohbati, R.: A robust feldspar luminescence dating method for Middle and Late Pleistocene sediments, Boreas, 41, 435–451, 2012.

Forman, S. L., Pierson, J., Gomez, J., Brigham-Grette, J. Nowaczyk, N. R., and Melles, M.: Luminescence geochronology for sediments from Lake El'gygytgyn, Northeast Siberia, Russia: constraining the timing of paleoenvironmental events for the past 200 ka, J. Paleolimnol., 37, 77–88, 2007.

Fuchs, M. and Owen, L. A.: Luminescence dating of glacial and associated sediments: review, recommendations and future directions, Boreas, 37, 636–659, 2008.
Frechen, M, Schweitzer, U., and Zander, A.: Improvements in sample preparation for the fine grain technique, Ancient TL, 14, 15–17, 1996.
Huntley, D. J. and Lamothe, M.: Ubiquity of anomalous fading in K-feldspars and the measurement and correction for it in optical dating, Can. J. Earth Sci., 38, 1093–1106, 2001.
Jacobs, Z., Roberts, R. G., Lachlan, T. J., Karkanas, P., Marean, C. W., and Roberts, D.: Development of the SAR TT-OSL procedure for dating Middle Pleistocene dune and shallow marine deposits along the southern Cape coast of South Africa, Quat. Geochronol., 6, 491–513, 2011.
Juschus, O., Preusser, F., Melles, M., and Radtke, U.: Applying SAR-IRSL methodology for dating fine-grained sediments from Lake El'gygytgyn, North-Eastern Siberia, Quat. Geochronol., 2, 187–194, 2007.
Krbetschek, M. R., Rieser, U., Zöller, L., and Heinicke, J.: Radioactive disequilibria in palaeodosimetric dating of sediments, Radiat. Meas., 23, 485–489, 1994.
Lai, Z. P.: Chronology and the upper dating limit for loess samples from Luochuan section in the Chinese Loess Plateau using quartz OSL SAR protocol, J. Asian Earth Sci., 37, 176–185, 2010.
Lamothe, M. and Auclair, M.: A solution to anomalous fading and age shortfalls in optical dating of feldspar minerals, Earth Planet. Sc. Lett., 171, 319–323, 1999.
Li, B. and Li, S. H.: Luminescence dating of K-feldspar from sediments: a protocol without anomalous fading correction, Quat. Geochronol., 6, 468–479, 2011.
Lowick, S. and Preusser, F.: A method for retrospectively calculating water content for desiccated core samples, Ancient TL, 27, 9–14, 2009.
Lowick, S. and Preusser, F.: Investigating age underestimation in the high dose region of optically stimulated luminescence using fine grain quartz, Quat. Geochronol., 6, 33–41, 2011.
Lowick, S., Preusser, F., Pini, R., and Ravazzi, C.: Underestimation of fine grain quartz OSL dating towards the Eemian: comparison with palynostratigraphy from Azzano Decimo, Northeastern Italy, Quat. Geochronol., 5, 583–590, 2010.
Lukas, S., Preusser, F., Anselmetti, D. S., and Tinner, W.: Testing the potential of luminescence dating of high-alpine lake sediments, Quat. Geochronol., 8, 23–32, 2012.
Melles, M., Brigham-Grette, J., Glushkova, O. Yu., Minyuk, P. S., Nowaczyk, N. R., and Hubberten, H.-W.: Sedimentary geochemistry of core PG1351 from Lake El'gygytgyn – a sensi-

CPD
8, 4779–4815, 2012

tive record of climate variability in the East Siberian Arctic during the past three glacialinterglacial cycles, J. Paleolimnol., 37, 89–104, 2007.
Melles, M., Brigham-Grette, J., Minyuk, P., Koeberl, C., Andreev, A., Cook, T., Fedorov, G., Gebhardt, C., Haltia-Hovi, E., Kukkonen, M., Nowaczyk, N., Schwamborn, G., Wennrich, V., and the El'gygytgyn Scientific Party: The Lake El'gygytgyn scientific drilling project – conquering Arctic challenges through continental drilling, Scientific Drilling, 11, 29–40, doi:10.2204/iodp.sd.11.03.2011, 2011.
Melles, M., Brigham-Grette, J., Minyuk, P. S., Nowaczyk, N. R., Wennrich, V. DeConto, R. M., Anderson, P. M. Andreev, A. A., Coletti, A. Cook, T. L., Haltia-Hovi, E., Kukkonen, M., Lozhkin, A. V., Rosén, P., Tarasov, P., Vogel, H., and Wagner, B.: 2.8 million years of Arctic climate change from Lake El'gygytgyn, NE Russia, Science, 337, 315–320, doi:10.1126/science.1222135, 2012.
Murray, A. S. and Wintle, A. G.: Luminescence dating of quartz using an improved single-aliquot regenerative-dose protocol, Radiat. Meas., 32, 57–73, 2000.
Murray A. S., Buylaert, J. P., Henriksen, M., Svendsen, J. I., and Mangerud, J.: Testing the reliability of quartz OSL ages beyond the Eemian, Radiat. Meas., 43, 776–780, 2008.
Nolan, M., Liston, G., Prokein, P., Brigham-Grette, J., Sharpton, V., and Huntzinger, R., Analysis of lake ice dynamics and morphology on Lake El'gygytgyn, Siberia, using SAR and Landsat, J. Geophys. Res., 108, 8062, doi:10.1029/2001JD000934, 2002.
Nowaczyk, N., Wennrich, V., Melles, M., Brigham, J., and El'gygytgyn Scientific Party: Detailed age model for upper 125 m of core D1 from Lake El'gygytgyn, NE Russia, as derived from orbital forcing, Clim. Past Discuss., in preparation, 2012.
Porat, N., Duller, G. A. T., Roberts, H. M., and Wintle, A. G.: A simplified SAR protocol for TT-OSL, Radiat. Meas., 44, 538–542, 2009.
Preusser, F., Ramseyer, K., and Schlüchter, C.: Characterisation of low OSL intensity quartz from the New Zealand Alps, Radiat. Meas., 41, 871–877, 2006.
Rees-Jones, J.: Optical dating of young sediments using fine-grain quartz, Ancient TL, 13, 9–14, 1995.
Stevens, T., Buylaert, J.-P., and Murray, A. S.: Towards development of a broadly-applicable SAR TT-OSL dating protocol for quartz, Radiat. Meas., 44, 639–645, 2009.
Thiel, C., Buylaert, J.-P., Murray, A. S., Terhorst, B., Hofer, I., Tsukamoto, S., and Frechen, M.: Luminescence dating of the Stratzing loess profile (Austria) – testing the potential of an elevated temperature post-IR IRSL protocol, Quaternary Int., 234, 23–31, 2011.

CPD
8, 4779–4815, 2012

Testing the potential of OSL, TT-OSL, IRSL and post-IR IRSL luminescence dating

A. Zander and A. Hilgers

Thomsen, K. J., Murray, A. S., Jain, M., and Bøtter-Jensen, L.: Laboratory fading rates of various luminescence signals from feldspar-rich sediment extracts, Radiat. Meas., 43, 1474–1486, 2008.

Timar, A., Vandenberghe, D., Panaiotu, E. C., Panaiotu, C. G., Necula, C., Cosma, C., and Van den Haute, P.: Optical dating of Romanian loess using fine-grained quartz, Quat. Geochronol., 5, 143–148, 2010.

Tsukamoto, S., Duller, G. A. T., and Wintle, A. G.: Characteristics of thermally transferred optically stimulated luminescence (TT-OSL) in quartz and its potential for dating sediments, Radiat. Meas., 43, 1204–1218, 2008.

Wallinga, J., Murray, A. S., and Wintle, A. G.: The single aliquot regenerative-dose (SAR) protocol applied to coarse-grain feldspar, Radiat. Meas., 32, 529–533, 2000.

Wang, X. L., Wintle, A. G., and Lu, Y. C.; Thermally transferred luminescence in fine-grained quartz from Chinese loess: basic observations, Radiat. Meas., 41, 649–658, 2006.

Wang, X. L., Wintle, A. G., and Lu, Y. C.: Testing a single-aliquot protocol for recuperated OSL dating, Radiat. Meas., 42, 380–391, 2007.

Wennrich, V., Minyuk, P., Borkhodoev, V., Francke, A., Ritter, B., Raschke, U., Nowaczyk, N., Schwamborn, G., Brigham-Grette, J., Melles, M., and El'gygytgyn Science Party: Pliocene to Pleistocene climate and environmental history of Lake El'gygytgyn/NE Russia based on high-resolution inorganic geochemistry data, Clim. Past Discuss., in preparation, 2012.

Wintle, A. G.: Anomalous fading of thermoluminescence in mineral samples, Nature, 245, 143–144, 1973.

Table 1. Results of dose-rate determination using high-resolution gamma-ray spectrometry. Samples marked with an asterisk were measured at the VKTA Rossendorf e.V. The other 5 samples were measured at the luminescence laboratory in Cologne. Water content 1 was measured by drying the bulk sediment finally used for dose rate measurements and water content 2 was measured at a second correlative core soon after drilling. Water content 2 was later used for age calculations. All water content values are quoted as weight water/weight dry sediment. All values are presented with their 1-sigma error.

Lab. Code	Sample ID	Composite depth (m)	Field depth (m)	Water content (weight-%) 1	Water content (weight-%) 2	U (ppm)	Th (ppm)	K (%)
C-L3131	1A1H2	6.487–6.587	3.76–3.86	90.3	94.7	3.36 ± 0.18	12.40 ± 0.72	2.42 ± 0.09
C-L3132	1A1H3	7.469–7.569	4.77–4.87	30.9	122.0	3.33 ± 0.17	12.13 ± 0.70	2.34 ± 0.09
C-L2843	1B2H2*	11.09–11.19	8.32–8.42	72.5	52.9	4.30 ± 0.30	11.80 ± 0.40	2.39 ± 0.08
C-L3133	1A3H1	11.694–11.794	8.88–8.98	45.0	42.8	2.47 ± 0.13	10.46 ± 0.60	1.94 ± 0.08
C-L3134	1A3H2	12.596–12.696	9.815–9.915	69.3	74.8	3.08 ± 0.16	12.32 ± 0.71	2.42 ± 0.09
C-L3135	1B3H2	14.169–14.269	11.319–11.419	66.0	67.4	2.85 ± 0.15	11.75 ± 0.68	2.24 ± 0.09
C-L3136	1A4H2	15.626–15.726	12.79–12.89	73.8	70.5	6.17 ± 0.32	13.21 ± 0.77	2.53 ± 0.10
C-L2844	1A6H1B*	20.869–20.969	17.88–17.98	59.2	61.0	4.20 ± 0.30	12.40 ± 0.40	2.45 ± 0.08
C-L2845	1A9H2*	31.05–31.15	27.817–27.917	67.2	61.5	3.90 ± 0.40	12.70 ± 0.40	2.49 ± 0.08

CPD
8, 4779–4815, 2012

Testing the potential of OSL, TT-OSL, IRSL and post-IR IRSL luminescence dating

A. Zander and A. Hilgers

Table 2. Compilation of measurement protocols used in this study.

	OSL[a]	TT-OSL[b]	TT-OSL modified[c]	$IRSL^{d}_{50}$	$pIRIR^{e}_{290}$
1	Dose	Dose	Dose	Dose	Dose
2	Pre-heat 240 °C, 10 s	Pre-heat (200 °C, 10 s)	Pre-heat (200 °C, 10 s)	Pre-heat (270 °C, 10 s)	Pre-heat (320 °C, 60 s)
3	OSL (125 °C, 50 s) → L_x	OSL (125 °C, 300 s) → L_x	OSL (125 °C, 300 s) → L_x	IRSL (50 °C, 350 s) → L_x	IRSL (50 °C, 200 s → $L_{x\ \mathrm{IRSL\ 50}}$
4	Test dose	Pre-heat (260 °C, 10 s)	Pre-heat (260 °C, 10 s)	Test dose	IRSL (290 °C, 200 s) → $L_{x\ \mathrm{pIR\ 290}}$
5	Pre-heat (220 °C, 0 s)	OSL (125 °C, 100 s) → $L_{x\ \mathrm{TT}}$	OSL at 125 °C, 100 s → $L_{x\ \mathrm{TT}}$	Pre-heat (270 °C, 10 s)	Test dose
6	OSL (125 °C, 50 s) → T_x	Test dose	Heat to 300 °C, 100 s	IRSL (50 °C, 350 s) → T_x	Pre-heat (320 °C, 60 s)
7	Return to 1	Pre-heat (220 °C, 10 s)	Give test dose	Return to 1	IRSL (50 °C, 200 s) → $T_{x\ \mathrm{IRSL\ 50}}$
8		OSL at 125 °C, 100 s → T_x	Pre-heat (220 °C, 10 s)		IRSL (290 °C, 200 s) → $T_{x\ \mathrm{pIR\ 290}}$
9		Heat (300 °C, 100 s)	OSL (125 °C, 100 s) → T_x		IRSL (325 °C, 100 s)
10		Return to 1	Heat (300 °C, 100 s)		Return to 1
11			Return to 1		

[a] After Murray and Wintle (2000), [b] after Porat et al. (2009), [c] after Stevens et al. (2009), [d] after Wallinga et al. (2000), [e] after Thiel et al. (2011).

CPD
8, 4779–4815, 2012

Testing the potential of OSL, TT-OSL, IRSL and post-IR IRSL luminescence dating

A. Zander and A. Hilgers

Table 3. SAR-OSL dating results and multiple aliquot regenerative dose (MAR) TT-OSL dating results obtained on fine grain quartz (4–11 µm). Ages and dose rates are given for different assumed and the measured water content (weight-%) to point out the significance of the water content on the age estimates. All analytical results are presented with their 1-sigma error.

Sample ID	Composite depth (m)	Protocol	Number of sub-samples	RSD	Mean recycling ratio	Mean recuperation (%)	D_e (Gy)
1B2H2	11.09–11.19	SAR-OSL	6	5.0	1.01	0.9	380 ± 23
1A6H1B	20.869–20.969	SAR-OSL	8	25.1	0.99	1.4	404 ± 47
1A9H2	31.05–31.15	SAR-OSL	7	5.8	1.00	2.9	376 ± 22
1A1H3	7.469–7.569	TT-OSL	16				408 ± 35
1A4H2	15.626–15.726	TT-OSL	12				485 ± 34

Sample ID	Expected age[a] (ka)	Protocol	OSL age (ka) Water content assumed for age calculation				Dose rate ($Gy\,ka^{-1}$) Water content assumed for age calculation			
			measured	50 %	70 %	90 %	measured	50 %	70 %	90 %
1B2H2	~ 218	SAR-OSL	123 ± 13	121 ± 12	139 ± 15	158 ± 17	3.1 ± 0.3	3.1 ± 0.3	2.7 ± 0.2	2.4 ± 0.2
1A6H1B	~ 465	SAR-OSL	137 ± 20	126 ± 18	146 ± 21	165 ± 24	2.9 ± 0.3	3.2 ± 0.3	2.8 ± 0.2	2.4 ± 0.2
1A9H2	~ 757	SAR-OSL	129 ± 13	118 ± 12	136 ± 14	155 ± 16	2.9 ± 0.3	3.2 ± 0.3	2.8 ± 0.2	2.4 ± 0.2
1A1H3	~ 168	TT-OSL	216 ± 27	139 ± 16	161 ± 19	182 ± 22	1.9 ± 0.2	2.9 ± 0.2	2.5 ± 0.2	2.2 ± 0.2
1A4H2	~ 320	TT-OSL	151 ± 18	131 ± 15	151 ± 17	171 ± 20	3.2 ± 0.3	3.7 ± 0.3	3.2 ± 0.3	2.8 ± 0.3

[a] Inferred from Melles et al. (2012) and Nowaczyk et al. (2012)

CPD
8, 4779–4815, 2012

Table 4. Results of the pIRIR$_{290}$ bleaching experiments.

Sample ID	Composite depth (m)	Bleaching source	Time (min)	Post-IR IRSL residual	IRSL resdiual
1A1H2	6.487–6.587	Sunlight	450	14.4 ± 1.2 Gy	6.4 ± 0.6 Gy
1A1H2	6.487–6.587	Sunlight	195	20.1 ± 1.1 Gy	12.6 ± 1.0 Gy
1A3H1	11.694–11.794	Solar simulator	2160	13.7 ± 0.7 Gy	7.0 ± 0.4 Gy
1A3H2	12.596–12.696	Solar simulator	390	17.7 ± 1.0 Gy	9.9 ± 0.8 Gy
1A9H2	31.05–31.15	Solar simulator	270	11.5 ± 1.8 Gy	6.8 ± 0.9 Gy

CPD
8, 4779–4815, 2012

Table 5. Equivalent doses calculated for the post-IR IRSL signal measured at 290 °C and the IRSL signal measured at 50 °C in the course of the $pIRIR_{290}$ measurement sequence (see Table 2). All analytical results are presented with their 1-sigma error.

Sample ID	Composite depth (m)	Number of discs[a]	RSD (%)	IRSL D_e (Gy)	Number of discs[a]	RSD (%)	$pIRIR_{290}$ D_e (Gy)[b]
1A1H2	6.487–6.587	4/5	13	268 ± 27	4/5	7	464 ± 31
1A1H3	7.469–7.569	11/13	12	310 ± 23	12/13	12	625 ± 39
1A3H1	11.694–11.794	4/5	16	380 ± 45	4/5	8	955 ± 73
1A3H2	12.596–12.696	3/8	8	361 ± 24	5/8	28	983 ± 151
1B3H2	14.169–14.269	4/5	10	505 ± 40	5/5	9	1023 ± 84
1A4H2	15.626–15.726	5/9	15	395 ± 23	9/9	29	1242 ± 230
1A6H1B	20.869–20.969	6/6	16	540 ± 68	6/6	18	1629 ± 184
1A9H2	31.05–31.15	3/5	8	511 ± 35	4/5	11	> 2400

[a] Number of discs taken for D_e determination and total number of discs measured.
[b] Relating to the bleaching experiments, the residual signal equivalent to 20 Gy was subtracted from the D_e.

CPD
8, 4779–4815, 2012

Table 6. Results of the post-IR IRSL protocol. Note, that all IRSL results presented here are based on the IRSL measurements at 50 °C conducted as part of the $pIRIR_{290}$ protocol (see Table 2). Ages and dose rates are given for various assumed and the measured water contents. All analytical results are presented with their 1-sigma error.

Sample ID	Composite depth (m)	Expected age (ka)*	IRSL age (ka) Water content assumed for age calculation				$pIRIR_{290}$ age (ka) Water content assumed for age calculation				Dose rate (Gy ka^{-1}) Water content assumed for age calculation			
			measured	50 %	70 %	90 %	measured	50 %	70 %	90 %	measured	50 %	70 %	90 %
1A1H2	6.487–6.587	~ 145	103 ± 14	77 ± 10	89 ± 11	101 ± 13	179 ± 20	134 ± 14	154 ± 16	174 ± 19	2.6 ± 0.2	3.5 ± 0.3	3.0 ± 0.2	2.7 ± 0.2
1A1H3	7.469–7.569	~ 168	141 ± 17	92 ± 10	106 ± 12	119 ± 14	283 ± 31	185 ± 19	213 ± 22	240 ± 25	2.2 ± 0.2	3.4 ± 0.3	2.9 ± 0.2	2.6 ± 0.2
1A3H1	11.694–11.794	~ 227	131 ± 19	138 ± 20	159 ± 23	179 ± 26	329 ± 36	348 ± 38	400 ± 45	451 ± 52	2.9 ± 0.2	2.7 ± 0.2	2.4 ± 0.2	2.1 ± 0.2
1A3H2	12.596–12.696	~ 247	127 ± 13	107 ± 11	123 ± 13	139 ± 15	346 ± 60	292 ± 50	335 ± 58	378 ± 66	2.8 ± 0.2	3.4 ± 0.3	2.9 ± 0.2	2.6 ± 0.2
1B3H2	14.169–14.269	~ 295	181 ± 21	161 ± 18	185 ± 21	208 ± 24	368 ± 43	325 ± 36	374 ± 43	422 ± 50	2.8 ± 0.2	3.1 ± 0.2	2.7 ± 0.2	2.4 ± 0.2
1A4H2	15.626–15.726	~ 320	104 ± 11	90 ± 9	104 ± 11	117 ± 13	327 ± 68	284 ± 58	326 ± 67	368 ± 76	3.8 ± 0.3	4.4 ± 0.4	3.8 ± 0.3	3.4 ± 0.3
1A6H1B	20.869–20.969	~ 465	158 ± 24	146 ± 22	167 ± 25	189 ± 29	476 ± 67	439 ± 61	505 ± 72	570 ± 82	3.4 ± 0.3	3.7 ± 0.3	3.2 ± 0.3	2.9 ± 0.3
1A9H2	31.05–31.15	~ 757	151 ± 16	139 ± 15	160 ± 18	180 ± 20	> 700	> 650	> 750	> 850	3.4 ± 0.3	3.7 ± 0.3	3.2 ± 0.3	2.8 ± 0.2

* Inferred from Melles et al. (2012) and Nowaczyk et al. (2012).

Discussion Paper | Discussion Paper | Discussion Paper | Discussion Paper |

CPD

8, 4779–4815, 2012

Testing the potential of OSL, TT-OSL, IRSL and post-IR IRSL luminescence dating

A. Zander and A. Hilgers

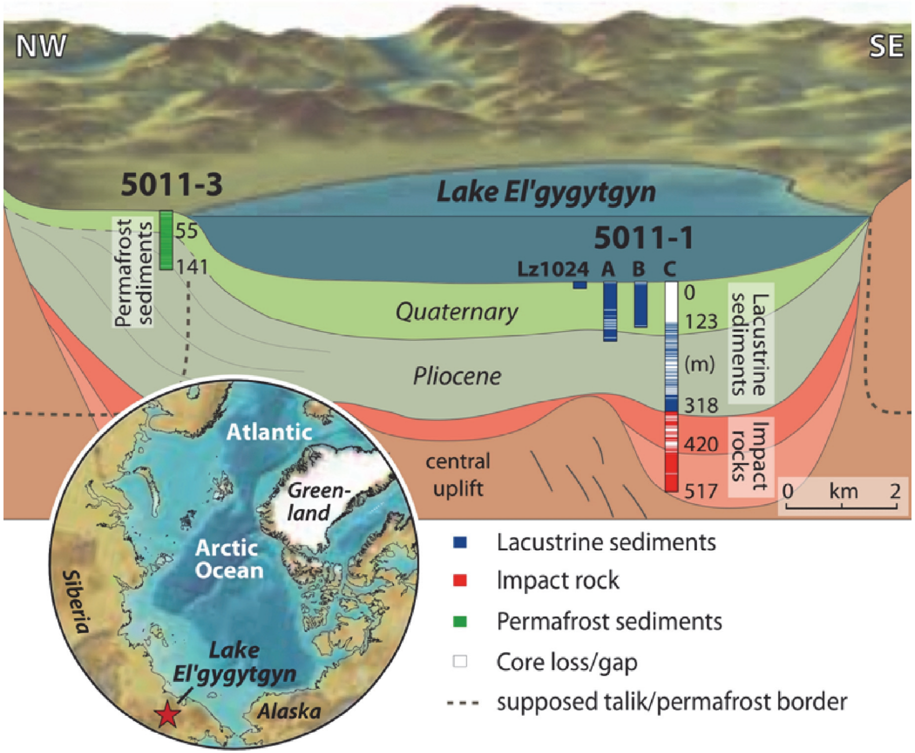

Fig. 1. Location of Lake El'gygytgyn in Northeastern Russia (inserted map) and schematic cross-section of the El'gygytgyn basin stratigraphy showing the location of ICDP Sites 5011-1 and 5011-3. Lz1024 is a 16-m long percussion piston core taken in 2003 that fills the stratigraphic gap between the lake sediment surface and the top of drill cores 1A and 1B (from Melles et al., 2012).

CPD
8, 4779–4815, 2012

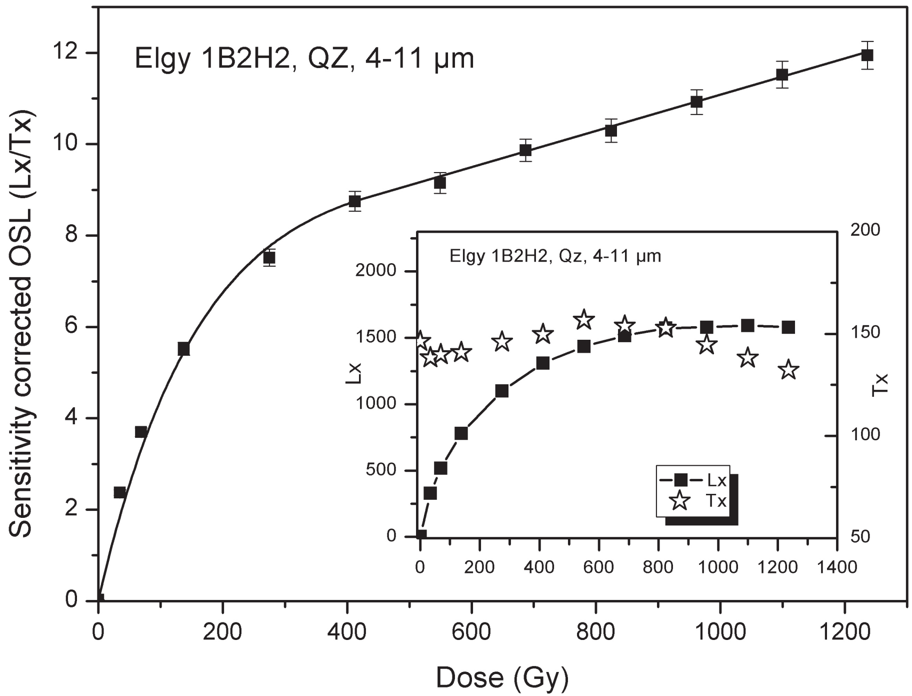

Fig. 2. Saturation dose curve of sample Elgy1B2H2. The standard SAR protocol was applied with 12 dose steps up to a maximum beta dose of 1237 Gy. Up to about 400 Gy the dose response signal is best fitted to an exponential function and then beyond to a linear function up to 1237 Gy. The inset shows that the background subtracted OSL regenerative curve is in saturation but a decreasing test dose signal results in a linear increase of the dose response curve.

CPD
8, 4779–4815, 2012

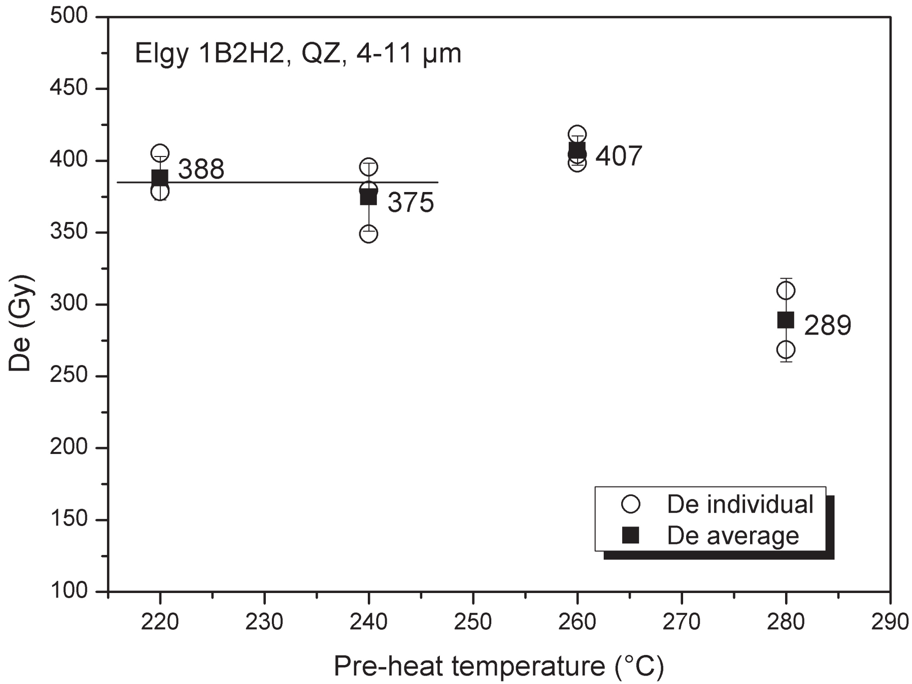

Fig. 3a. Validation of protocol parameters. A pre-heat plateau test at sample 1B2H2, carried out to define the appropriate pre-heat temperature. Three sub-samples of fine grain quartz were measured per temperature step and the resulting D_e plotted against the temperature. A 240/220 °C pre-heat/cut heat was chosen for further experiments with the SAR protocol.

CPD
8, 4779–4815, 2012

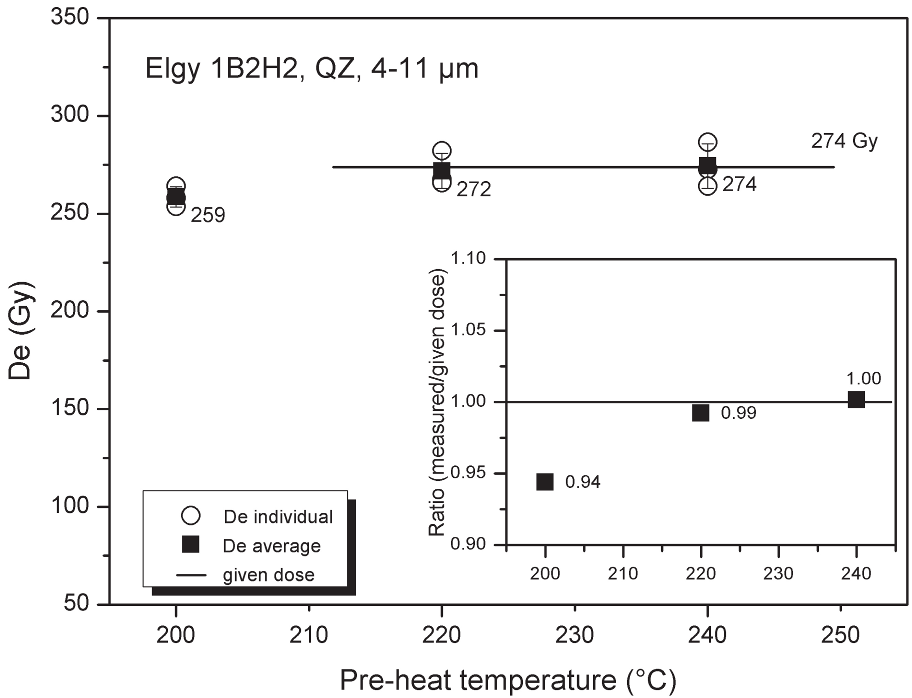

Fig. 3b. A dose recovery test combined with a pre-heat plateau for fine grain quartz. Samples were first bleached by a 100 s shine down at 125 °C to reset the natural luminescence signal and then irradiated with a 274 Gy beta dose. Three sub-samples each were measured at three different temperatures and yielded a perfect match at 240 °C with the given dose (ratio is 1.00, see inset), if the exponential plus linear function is fitted for D_e determination.

CPD
8, 4779–4815, 2012

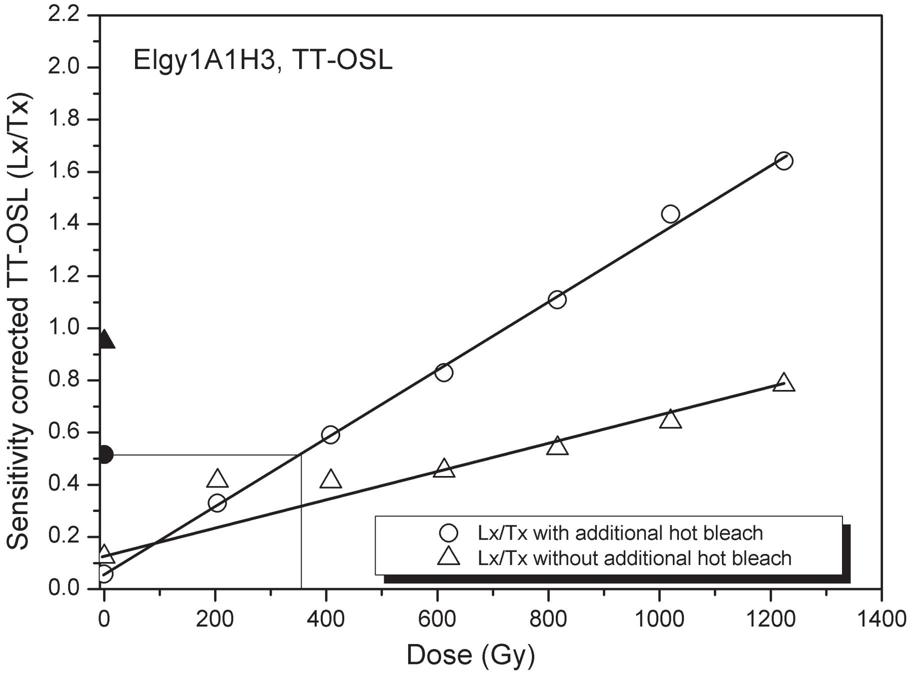

Fig. 4. Result of the modified SAR-TT-OSL (applied to fine grain quartz) protocol after Porat et al. (2009) before (triangles) and after (circles) adding an additional hot bleach before the test dose measurement.

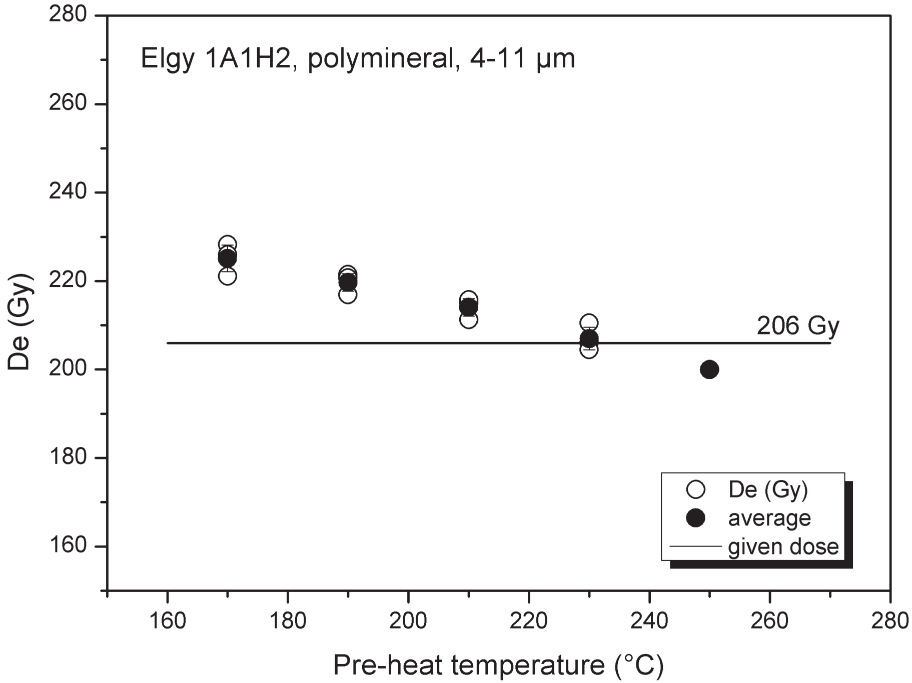

Fig. 5. Dose recovery pre-heat plot on sample 1A1H2 with the SAR $IRSL_{50}$ protocol. It was not possible to define a pre-heat plateau and the standard SAR $IRSL_{50}$ protocol was abandoned.

CPD
8, 4779–4815, 2012

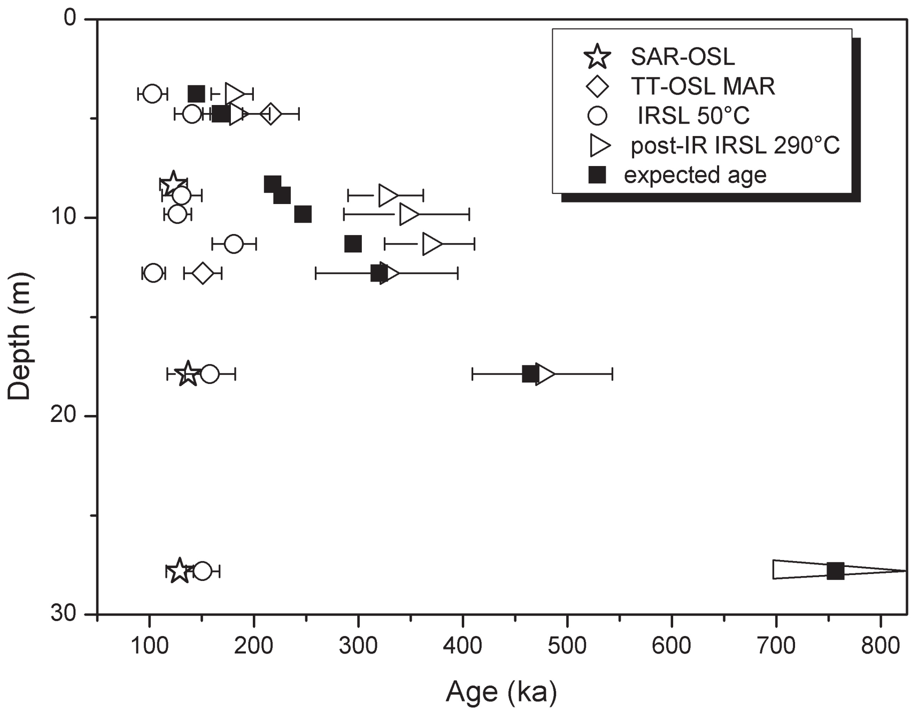

Fig. 6. Comparison of the expected ages from an independent age model (Melles et al., 2012; Nowaczyk et al., 2012) and luminescence ages determined with different luminescence dating protocols on fine grain quartz and on polymineral fine grain. The graph shows the luminescence ages which were calculated with the measured water content. The extended triangle in the lower right corner correlates with the sample from the B/M boundary and is a symbol for the $pIRIR_{290}$ age of > 700 ka.

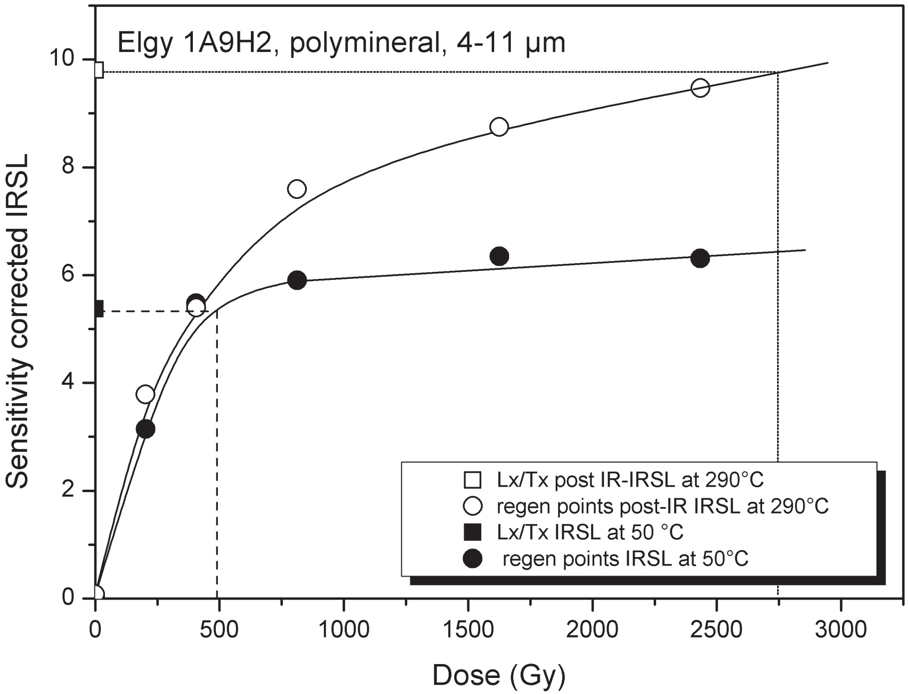

Fig. 7. Dose response curves for the IRSL signals measured at 50 °C and 290 °C, respectively, throughout the pIRIR$_{290}$ measurement sequence applied to polymineral fine grain extracts from sample 1A9H2, which is correlated to the B/M boundary.

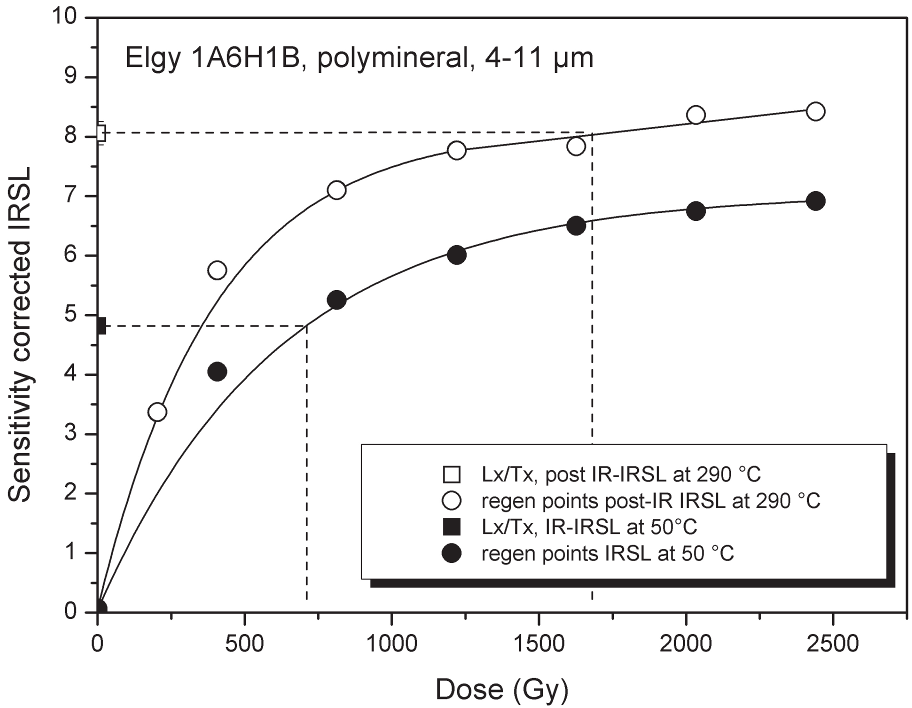

Fig. 8. Dose response curves for the IRSL signals measured at 50 °C and 290 °C, respectively, throughout the pIRIR$_{290}$ measurement sequence applied to polymineral fine grain extracts from sample 1A6H1B. The natural pIRIR signal (L_x/T_x) is already in the very flat linear part of the dose response curve which is approaching the saturation level. This fact substantially limits the precision of pIRIR$_{290}$ D_e determination.

CPD
8, 4779–4815, 2012

Testing the potential of OSL, TT-OSL, IRSL and post-IR IRSL luminescence dating

A. Zander and A. Hilgers